LES OF A TWO-PHASE TURBULENT STIRRED REACTOR

Zhilei Wu
Div. of Fluid Mechanics, Lund Institute of Technology
SE-221 00 Lund, Sweden
Zhilei.Wu@vok.lth.se

Johan Revstedt
Div. of Fluid Mechanics, Lund Institute of Technology
SE-221 00 Lund, Sweden
Johan.Revstedt@vok.lth.se

Laszlo Fuchs
Div. of Fluid Mechanics, Lund Institute of Technology
SE-221 00 Lund, Sweden
Laszlo.Fuchs@vok.lth.se

ABSTRACT

LES of a baffled stirred reactor in the presence of bubbles is performed. A multi-grid finite difference code using staggered Cartesian grid is used. The rotating impeller blades are modelled by adding source terms to the Navier-Stokes equations. Euler-Lagrangian approach is used to simulate the two-phase flow, i.e. bubbles are tracked in the turbulent flow field. The effect of bubbles on the properties of the continuous phase are investigated. Two-way coupling simulations with a gas volume fraction of 0.5% are performed and compared to simulations of single phase liquid flow. The results show that the presence of bubbles decrease the averaged radial and azimuthal liquid velocity at the blade tip. This result is in agreement with published experimental data. Also, when the two-way coupling effect is taken into account, the trailing vortices of the blade are decreased in strength.

INTRODUCTION

Stirred reactors are widely used in chemical and biochemical industries. The role of the stirrer is to enhance mixing by increased convective transport on large scales and high level of turbulence for small scale mixing. The flow structure of the stirred reactor is complex, in the vicinity of the impeller the flow is highly turbulent and the structure is very much like a radial swirling jet, when studied in a fixed frame of reference. There is however a strong periodic behaviour closely associated with the flow close to the impeller blades. A pair of trailing vortices originating behind these blades are responsible for the periodic fluctuations (van't Riet and Smith, 1975). Further away from the impeller the flow is dominated by large scale slowly varying structures (Ståhl-Wernersson and Trägårdh, 1999).

When simulating flows in stirred reactors one has not only to consider how to model turbulence but also how to describe the motion of the turbine blades. Methods for this can be divided into two major groups depending on the grid structure used. One may consider using a combination of moving and stationary grids, i.e. the reactor is described on a stationary grid and a rotating grid is attached to the impeller. However, in conjunction with LES on a Cartesian grid it is more feasible to use a stationary grid approach. Although, the boundary conditions becomes more complex. A suitable way to represent the effect of the turbine on the fluid is to add source terms to the momentum equations at the positions where the blades are located and moving the sources along with the turbine rotation. This approach has been used successfully together with LES in the studies by Eggels (1996), Derksen and van den Akker (1999) and Revstedt et al. (1998), (2000).

Most of the simulation work on stirred vessels has been focused on single phase flows. In many industrial process, two phase gas-liquid flows in stirred vessels is encountered. When the gas phase is introduced into the system, the flow becomes more complex due to the interaction between the gas and the liquid. This interaction leads among other things to dispersion of to the bubbles as well as changes in the flow properties of the liquid phase. Experiments, e.g. by Ranade (2000), show that the presence of the bubbles alters the flow around the impeller blades. This in turn affects the distribution of the bubbles.

The attempts to simulate gas-liquid flows within stirred vessels are relatively few. One-way coupling (the bubbles are affected by the flow but the flow is assumed to be unaffected by the bubble) have been carried out by Bakker and van den Akker (1992). They use detailed single-phase flow simulations to track the movement of bubbles in gas-liquid vessels. Gosman et al. (1992) have used a complete two-fluid model to simulate gas-liquid flow in stirred vessels. Ranade and van den Akker (1994) have proposed a computational snapshot approach to simulate flow around impeller blades, which they applied for the simulation of gas-liquid stirred vessels. Friberg and Hjertager (1998), (1999) used an Eulerian two-fluid model to study gas-liquid flow in a industrial size stirred reactor.

In this work, Large Eddy Simulation is extended for handling of gas-liquid flows in stirred vessels. Under the assumption of low bubble volume fraction, the bubbles are tracked in the three-dimensional time-dependent flow field that is generated by LES, with reasonable computational effort. The aim of the present paper is to give a qualitative picture of how the presence of a gas phase alters the liquid flow in a stirred reactor.

GOVERNING EQUATIONS

LES is based on spatial filtering of the equations of motion. The space filtering of a function is defined as

$$\overline{\phi(x,t)} = \int_{-\infty}^{\infty} G(x-x')\,\phi(x',t)dx' \qquad (1)$$

Where ϕ is an arbitrary function and G is a filter function. The space filtered incompressible Naiver-Stokes equations can be written as:

$$\frac{\partial \overline{u_i}}{\partial x_i} = 0 \qquad (2)$$

$$\frac{\partial \overline{u_i}}{\partial t} + \overline{u_j}\frac{\partial \overline{u_i}}{\partial x_j} = -\frac{1}{\rho}\frac{\partial \overline{p}}{\partial x_i} + \nu\frac{\partial}{\partial x_j}\frac{\partial \overline{u_i}}{\partial x_j}i - \frac{\partial \tau_{ij}}{\partial x_j} + \overline{F_i} + \overline{F_{ib}} \qquad (3)$$

$$\tau_{ij} = \overline{u_i u_j} - \bar{u_i}\bar{u_j} \qquad (4)$$

where $\overline{F_i}$ and $\overline{F_{ib}}$ are source terms from the impeller and the bubbles, respectively. τ_{ij} is the Sub Grid Scale (SGS) stress tensor,which reflects the effect of unresolved scales on the resolved scales and has to be to be modelled. In this work, no explicit SGS model is applied (so called "implicit" SGS model). Of course, the implicit type of SGS model is appropriate only with adequately fine spatial resolution, i.e. such that the spatial resolution lies in the inertial subrange of the Kolmogorov energy cascade (c.f. Gullbrand et al. (1998)).

Lagrangian Particle Tracking (LPT) is performed to track individual bubbles in the three dimensional time dependent flow field that is generated by LES. The resulting force on each bubble may be decomposed into several contributions with different physical interpretation. Neglecting the Basset history force we get for a bubble with mass m_p and velocity v:

$$m_p\frac{dv_i}{dt} = (m_p - m_f)g_i + m_f\frac{Du_i}{Dt} - \frac{1}{2}m_f\left(\frac{du_i}{dt} - \frac{dv_i}{dt}\right) - 6\pi a\mu f(v_i - u_i) \qquad (5)$$

The right hand side of equation (5) includes a decomposition of the forces that act on the bubble. These are, the buoyancy, the pressure, the added mass and the drag.

In the drag term, a coefficient 'f ' is used to modify the drag force to be applicable for high Reynolds numbers. For spherical particles with particle Reynolds numbers below 1000, f can be approximated by an empirical correlation:

$$f = 1 + 0.15Re_p^{0.687} \qquad (6)$$

Where Re_p is the bubble Reynolds number based on its relative velocity magnitude $|\vec{u}_r| = |\vec{v} - \vec{u}|$and bubble diameter d:

$$Re_p = \frac{\rho\,|\vec{u}_r|\,d}{\mu} \qquad (7)$$

In the momentum equation of the continuous phase, a source term appears which is the force exerted by the bubbles on the continuous phase. This is consequence of two-way coupling. When one-way coupling is considered, this terms, is of course taken to be zero.

NUMERICAL METHOD

The spatial discretization of the governing equations is performed on a Cartesian staggered grid. The momentum and continuity equations are discretized using finite differences. A third order accurate upwind scheme (Kawamura and Kuwahara, 1984) is used for the convective terms and fourth order central scheme is used for the diffusive terms (Fuchs, 1984). The high-order schemes are not used directly in the approximation of the filtered equations since it may lead to a less robust solver. Instead, first a lower order scheme (first order for convective terms and second order for the others) to approximate the equations is used, then the high order terms are introduced as a 'single-step' defect correction to the lower order scheme (Fuchs, 1984). This approach takes advantage of both the efficiency of lower order schemes and the better accuracy of the higher order schemes. For smooth problems, this correction procedure is adequate to maintain the theoretical accuracy of the high order schemes. The time integration is done by a three-level implicit scheme. In each time step, the system of equations are solved using a multi-grid solver. The pressure-velocity coupling is handled by the Distributed Gauss-Seidel (DGS) method.

The equation of motion of the bubble is integrated by a second order Runge-Kutta scheme. In each time step, after the convergence of the flow field, the flow properties are interpolated to the bubble position. The forces on the bubbles are then calculated using the properties of the flow and the bubbles. The force information is used to update the bubble velocity and position. At every 5 time steps, the bubble velocity and position are recorded so as to collect samples for computing the statistical properties of the flow (such as velocity, void fraction, fluid-bubble velocity correlation).

SIMULATIONS

Simulations geometry and studied cases

The simulations are done on a water-filled cylindrical tank with two six-bladed Rushton impellers centred radially. The geometrical set-up and the coordinate system are shown in Figure 1. Bubbles are released at rest from small holes in a ring centred at the bottom of the tank. The diameter of the ring that used to introduce the bubbles is $D/4$,. The turbine speed is 300 rpm, corresponding to a Reynolds number of around 50,000.

In the simulations, three global grids and two locally refined grids around the position of each impeller are used. The finest global grid had $90 \times 42 \times 42$ nodes were and the finest local level had $26 \times 74 \times 74$ nodes.

Boundary conditions

The effects of the rotating impellers on the flow field are modelled by adding source terms to the momentum equations. The magnitude of these source terms is determined based on local velocity conditions (Revstedt and Fuchs, 2001). The impeller blades are thin and described as having sub-grid thickness. The implications of this are further discussed by Revstedt et al. (2000). No-slip conditions are set on the tank walls and on the baffles. The hubs and shaft of the Rushton turbine are neglected.

RESULTS

The Rushton impeller consists of a circular disc with six rectangular blades that will discharge the flow in the radial direction. The typical time averaged flow field of single-phase liquid flow using two Rushton impellers is shown in Figure 2. A pair of toroidal vortices are created for each impeller, recirculating the flow to the impeller region. As can be seen there is no mean mass transfer between the recirculation region for each impeller, this is often referred to as comparmentization. In this particular configuration it can be noted that in a fairly large volume above the upper impeller the flow is almost stagnant. If gas bubbles are introduced the the mean flow pattern will change somewhat (Figure 3). Two things are noticeable here, the upper recirculation vortex of the lower impeller is changed in shape and at what in the single-phase case was a sharp boundary between the impeller compartments there is now a clearly visible mean mass transport upwards. Also, the upper recirculation vortex of the upper impeller is larger in the two-phase case and we detect a higher velocity in the bulk region at the top. Responsible for these changes in liquid the flow field is, of course, the motion of the bubbles. Considering the mean gas velocity field (Figure 4) one can see that bubbles coming from the sparger at the bottom will be dispersed radially by the lower impeller. Some bubbles are then captured by the lower recirculation vortex, but most of them will be transported to the upper impeller. To get more details about the effects of the bubble on the liquid flow we study the mean velocity at the centre line of the impeller discharge. As seen in Figure 5 there is a substantial decrease in the radial and tangential velocity components, which is in agreement to the experimental data by Deen and Hjertager (1999). This is expected since the discharge flow is very dependent on the pressure difference over the blade, which is changed due to accumulation of gas on the suction side. The axial velocity is shown for both impellers and, as can be seen, close to the impeller we get a positive axial velocity for the two-phase case due to the bubble rising. However, close to the wall the velocity is negative, probably due to that the bubble motion will "lift" the whole radial jet.

Since the flow close to the impellers is strongly periodic it is of interest also to study the flow relative to the impeller. The angular resolved average of a function $g(\tau)$ can be defined as

$$\hat{g}(\tau) = \frac{1}{N} \sum_{n=0}^{N} g(\tau + nT) \tag{8}$$

where T denotes the period and N is the total number of samples. Due to spatial symmetry, the period T is specified as the time it takes for the impeller to turn 60^o. Data was sampled along the positive y-axis at time intervals corresponding to an impeller movement of 1^o. We hereby obtain data in a cylindrical coordinate system without having to interpolate from the Cartesian grid. Figure 6 shows the velocity field relative to the rotating impeller at the impeller centre plane. The impeller is rotating anti-clockwise and the blades are located at "12 o'clock" and at "2 o'clock". The major part of the discharge flow originates from just behind the blade. It is reported by Stoots and Calabrese (1995) the maximum radial velocity at the blade tip radius is at about 20° downstream of the blade. Here it is closer which is an effect of the impeller description. If one instead considers the flow in an axial-tangential plane within the volume swept by the impeller see the typical trailing vortices generated by the impeller blade. In the single phase case (Figure 7) these vortices are quite symmetrical. However, in the two-phase case (Figure 8) the structure is different, the vortices are no longer symmetrical and the boundary between them is shifted upwards.

CONCLUSIONS

Large Eddy Simulation of turbulent flows in a stirred reactor is extended to cases where bubbles are present. Lagrangian particle tracking is used to simulate the bubble motions in the flow field. It can be seen that introducing a relatively small amount of gas, in this case 0.5% per volume, will have a quite considerable influence on the liquid velocity field.

ACKNOWLEDGEMENTS

Financial support for this work was provided by the Swedish Strategic Research Foundation (SSF) through the Multi-phase Flow program.

REFERENCES

Bakker, A. and van den Akker, H.E.A., 1992, "A computational study on dispersing gas in a stirred reactor", *Fluid Mechanics of Mixing*, R. King, ed., Kluwer, Amsterdam.

Deen, N.G. and Hjertager, B.H., 1999, "Multiphase particle image velocimetry measurements in an aerated stirred tank", *Annual Meeting of the American Institute of Chemical Engineers.*

Derksen, J. and van den Akker, H.E.A., 1999, "Large eddy simulations on the flow driven by a Rushton turbine", *AIChE Journal*, Vol. 45, pp. 209-221.

Eggels, J.G.M., 1996, "Direct and large eddy simulations of turbulent fluid flow using the lattice-Boltzmann scheme", *int. J. Heat and Fluid Flow*, Vol. 17, pp. 307-323.

Friberg, P.C. and Hjertager, B.H., 1998, "Simulation of a 3-dimensional large-scale fermenter with four Rushton turbines using a two-fluid model", *Proc. of Third International Conference on Multi-phase Flows*, Lyon.

Friberg, P.C. and Hjertager, B.H., 1999, "Simulation of a 3-dimensional large-scale fermenter with four Rushton turbines", *Proc. of Second International Symposium on Two-Phase Flow Modelling and Experimentation*, Pisa.

Fuchs, L., 1984, "Defect-corrections and higher numerical accuracy", *Proc. of the GAMM-workshop on 'Efficient Solvers for Elliptic Systems', Notes on Numerical methods in Fluid Mechanics*, W. Hackbusch, ed., Vol. 10. pp 52-66.

Gosman, A.D., Lekakou, C., Politis, S., Issa, R.I. and Looney, M.K, 1992, "Multidimensional modeling of turbulent two-phase flows in stirred vessels", *AIChE Journal*,Vol. 38, pp1946-1956.

Gullbrand, J., Bai, X-S. and Fuchs, L., 1998, "Large eddy simulation of turbulent reacting flows using Cartesian grid and boundary corrections", *AIAA paper*, 98-3317.

Kawamura, T. and Kuwahara, K., 1984, "Computation of high Reynolds number flow around a circular cylinder with surface roughness", *AIAA paper*, 84-0340.

Ranade, V.V., 2000, "Influence of gas rate on structure of trailing vortices of a Rushton turbine: PIV measurement and CFD simulations", *14th int. Congress of Chemical and Process Engineering*, Paper No. 0600.

Ranade, V.V. and van den Akker, H.E.A., 1994, "Computational snapshot of gas-liquid flow in baffled stirred reactors", *Chemical Engineering Science*, Vol. 49, pp. 5175-5192.

Revstedt, J. and Fuchs, L., 2001, "Handling complex boundaries on a Cartesian grid using surface singularities", *int. J. Numer. Meth. Fluids*, Vol.35, pp. 125-150.

Revstedt, J., Fuchs, L. and Trägårdh, C., 1998, "Large eddy simulations of the turbulent flow in a stirred reactor", *Chemical Engineering Science*, Vol. 53, pp. 4041-4053.

Revstedt, J., Kovács, T., Fuchs, L. and Trägårdh, C., 2000, "Influence of impeller type on the flow structure in a stirred reactor", *AIChE Journal*, Vol. 46, pp. 2373-2382.

van't Riet, K. and Smith, J.M., 1975, "The trailing vortex system produced by Rushton turbine agitators", *Chemical Engineering Science*, Vol. 30, pp. 1093-1105.

Stoots, C.M. and Calabrese, R.V., 1995, "Mean velocity field relative to a Rushton turbine blade", *AIChE Journal*, Vol. 41, pp. 1-11.

Ståhl Wernersson, E. and Trägårdh, C., 1999, "Turbulence charateristics in turbine-agitated tanks of different size and geometries", *Chem. Eng. J.*, Vol. 72, pp. 97-107.

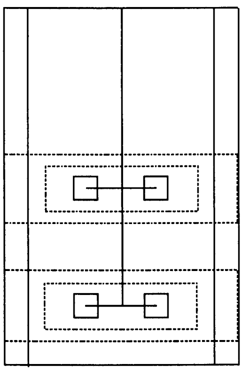

Figure 1: Schematic view of the computational geometry

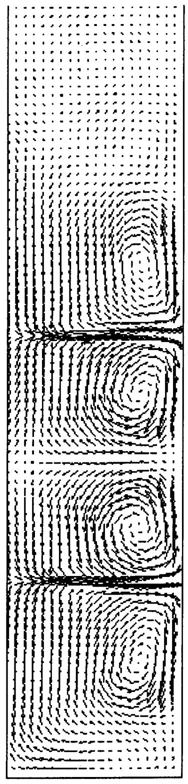

Figure 2: Time averaged velocity field in half of the centre plane (centre line to the left) for single-phase liquid flow.

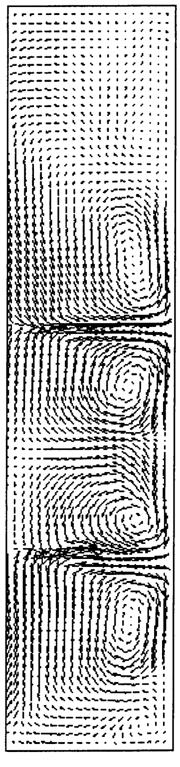

Figure 3: Time averaged liquid velocity field in half of the centre plane for gas-liquid flow.

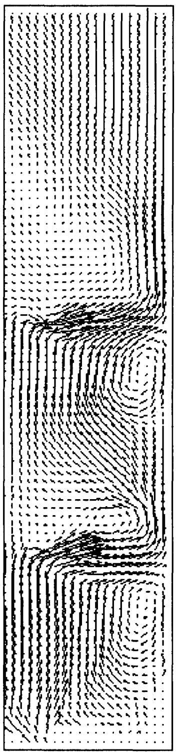

Figure 4: Time averaged bubble velocity field in half of the centre plane for gas-liquid flow.

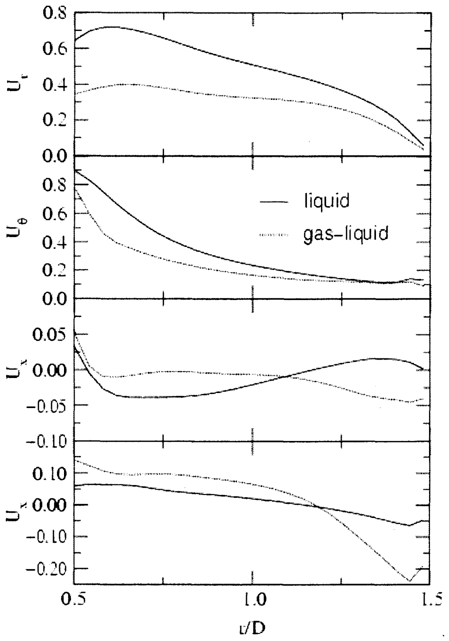

Figure 5: Time averaged liquid velocity in the centre line of the impeller discharge.

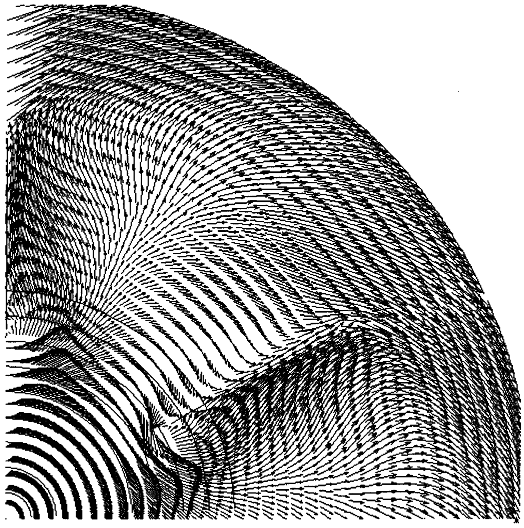

Figure 6: Angular resolved averaged liquid velocity field in the impeller centre plane (rotation is anti-clockwise).

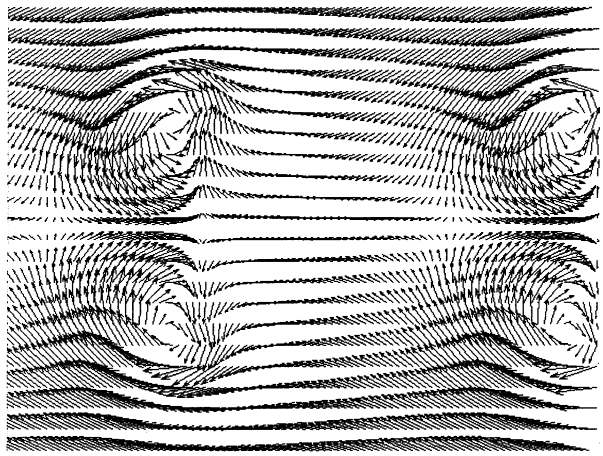

Figure 7: Angular resolved averaged velocity field for single-phase liquid flow in a axial-tangential plane in the volume swept by the impeller (the blades move from left to right).

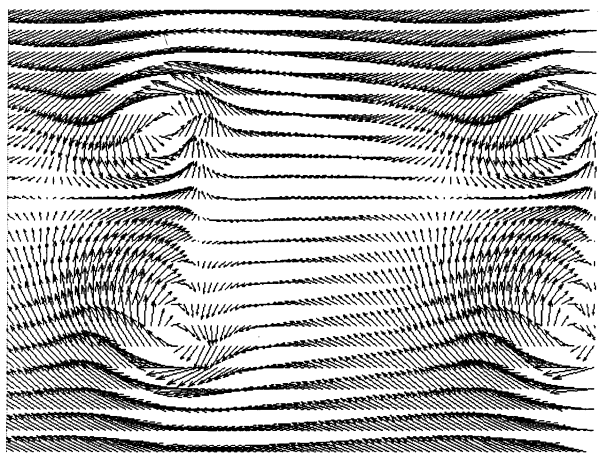

Figure 8: Angular resolved averaged liquid velocity field for gas-liquid flow in a axial-tangential plane in the volume swept by the impeller (the blades move from left to right).